Journal of Engineering Mathematics, Vol. 13, No. 3 July 1979

Implicit dissipative schemes for solving systems of conservation laws

D.N. HOLLA and P.C. JAIN

Department of Mathematics, Indian Institute of Technology, Powai, Bombay 400 076, India

(Received March 14, 1979)

SUMMARY

New implicit schemes for solving a system of conservation laws in one space dimension are obtained by using the cubic-spline technique. By making use of certain perturbation terms, these implicit schemes have been transformed to dissipative schemes. The nonlinear instabilities appearing in the solution in the narrow shock region have been damped by applying the automatic switched Shuman-filter method. Four test examples with continuous and discontinuous initial conditions have been solved to illustrate the theory. The proposed method has been extended to solve a system of conservation laws in two space dimensions.

1. Introduction

Nonlinear hyperbolic systems arise in several areas like gas dynamics, astrophysics and meteorology. In recent years, many finite-difference schemes have been proposed for solving these systems of conservation laws (cf. Richtmyer [1], Gourlay and Morris [2], Rubin and Burstein [3], McGuire and Morris [4]). As these schemes are explicit, they involve a severe restriction on the time step. Some implicit schemes (cf. Gourlay and Morris [5], Gary [6], Abarbanel and Zwas [7], Beam and Warming [8]) have also been proposed for solving these systems; these schemes are nondissipative. However, McGuire and Morris [9] have proposed a dissipative implicit finite-difference scheme of second order for solving such a system.

The order of accuracy in all these schemes ranges from order one to order four. Numerical results obtained by the first-order schemes show smooth profiles of discontinuities, resisting nonlinear instability; the shocks are found to be very smeared. The use of second- and higher-order schemes give rise to sharp profiles with large oscillations. These abnormal results are due to the presence of higher-order derivatives near shock-like discontinuities. The schemes of third and fourth order are of little practical value because of their complexity demanding an excessive use of computer time; they also do not provide any specific advantage in handling the discontinuities.

Implicit schemes, in general, are numerically more stable. They are more useful when the instability bound of the explicit scheme is more restrictive than the desired accuracy bound.

In the present paper, we have used the cubic-spline technique and certain perturbation terms for devising a general second-order dissipative implicit scheme. The dissipative nature of the scheme produces a damping for the smaller Fourier components but not for the selective components of the solution. In order to overcome this difficulty, we have used an automatic switched Shuman-filter to devise schemes which automatically and smoothly switch on the numerical filter only in the narrow shock region. The filter technique keeps the order of the original scheme unaltered in the smooth region. By choosing proper values of the parameters occurring in the general scheme, we have derived some schemes well-known from literature and a scheme of third-order accuracy. We have solved test examples to illustrate the merits of the schemes. The proposed numerical technique provides a unified treatment for deriving finite-difference schemes for the solution of systems of conservation laws.

2. The one-dimensional case

Consider the system of conservation laws

$$\frac{\partial u}{\partial t} + \frac{\partial f}{\partial x} = 0 \tag{2.1}$$

with the initial and boundary conditions

$$u(x, 0) = u_0(x), \qquad u(0, t) = u_1(t), \tag{2.2}$$

respectively, where $u = u(x, t)$ is a vector and $f = f(u)$ is a vector function. The solution is sought in the region

$$R = [0 \leqslant x \leqslant X] \times [t > 0].$$

The existence and uniqueness of the solution of this system are discussed by Jeffrey and Taniuti [10].

For the numerical solution of the problem, the region R is covered with grid points with mesh spacing h in the x-direction and time step k in the t-direction. We denote $u(ih, nk)$ by U_i^n. Then U_i^n and W_i^n denote the values of the solution of the differential equation and its finite-difference approximation respectively at the grid point (ih, nk). We take $X = Nh$, where N is the number of mesh points. Equation (2.1) is approximated as

$$W_i^{n+1} - W_i^n = k(\theta_1 m_i^{n+1} + \theta_2 m_i^n), \tag{2.3}$$

where $m_i^n = S_n'(x_i)$, $S_n(x)$ is the vector cubic-spline function interpolating $f_i (i = 0,1,2,...,N)$ at the nth time level, θ_1 and θ_2 are parameters. From the cubic-spline relations [11], we have

$$m_{i-1}^n + 4m_i^n + m_{i+1}^n = \frac{3}{h} \mu\delta f_i^n, \tag{2.4}$$

$$m_{i-1}^{n+1} + 4m_i^{n+1} + m_{i+1}^{n+1} = \frac{3}{h} \mu\delta f_i^{n+1}, \tag{2.5}$$

where $\mu\delta f_i^n = f_{i+1}^n - f_{i-1}^n$.

Eliminating m_i^n and m_i^{n+1} from Eqs. (2.3) to (2.5), an implicit finite-difference approximation to Eq. (2.1) is obtained in the form

$$\left(1 + \frac{\delta_x^2}{6}\right)(W_i^{n+1} - W_i^n) = \frac{p}{2}\,(\theta_1 \mu\delta f_i^{n+1} + \theta_2 \mu\delta f_i^n), \tag{2.6}$$

where $p = k/h$. This is the basic equation obtained from (2.1). We wish to develop a scheme which has at least second-order accuracy, is dissipative and has good stability properties. We perturb scheme (2.6) by the term $p\,(\overset{*}{f}{}^{n+a}_{i+\frac{1}{2}} - \overset{*}{f}{}^{n+a}_{i-\frac{1}{2}})$ with parameter a and adjust the parameters of the constituent terms. The modified form of scheme (2.6) is

$$\begin{aligned}\left(1 + \frac{b}{6}\delta_x^2\right)&(W_i^{n+1} - W_i^n)\\ &= \frac{p}{2}\left[\theta_1 \mu\delta f_i^{n+1} + \theta_2 \mu\delta f_i^n + 2c\,(\overset{*}{f}{}^{n+a}_{i+\frac{1}{2}} - \overset{*}{f}{}^{n+a}_{i-\frac{1}{2}})\right],\end{aligned} \tag{2.7}$$

where b and c are parameters and

$$\overset{*}{f}{}^{n+a}_{i} = f(\overset{*}{W}{}^{n+a}_{i}), \tag{2.8}$$

$$\overset{*}{W}{}^{n+a}_{i} = \frac{1}{2}(W^n_{i+\frac{1}{2}} + W^n_{i-\frac{1}{2}}) - ap(f^n_{i+\frac{1}{2}} - f^n_{i-\frac{1}{2}}). \tag{2.9}$$

It may be remarked that scheme (2.7) can also be obtained by the weighted linear finite-element method. By taking $b = 0$, $c = 0$, $\theta_1 = -1/2$ and $\theta_2 = -1/2$ in (2.7), one gets a scheme of Crank-Nicolson type. For $b = 0$ in (2.7), one gets the general scheme proposed by McGuire and Morris [9]; their scheme differs from (2.7) only in having the number of parameters reduced by one. Lerat and Peyret [12] have proposed a general explicit scheme for the system.

By using Taylor-series expansion about the point (ih, nk), we get four relations for the parameters a, b, c, θ_1, θ_2 in the form:

$$\theta_1 + \theta_2 + c = -1, \tag{2.10}$$

$$\theta_1 + ac = -1/2, \tag{2.11}$$

$$\theta_1 + a^2 c = -1/3, \tag{2.12}$$

$$\theta_1 + \theta_2 + \frac{c}{4} = -b. \tag{2.13}$$

Equations (2.10) and (2.11) give conditions for the scheme to be of second-order accuracy, while Eqs. (2.10) to (2.13) are the conditions for the scheme to be of third-order accuracy. Thus, we have obtained a three-parameter class of second-order accurate implicit schemes and a one-parameter class of third-order accurate implicit schemes for the given Eq. (2.1).

For examining the stability of these schemes, we eliminate the starred values from Eqs. (2.7) to (2.9). Using Fourier integrals, the linearized amplification matrix for (2.7) turns out to be

$$G(\alpha) = \frac{\left\{1 + \frac{b}{3}(\cos\alpha - 1) + \sqrt{-1}\ \bar{A}(\theta_2 + c)\sin\alpha - 2acp^2\bar{A}^2(\cos\alpha - 1)\right\}}{\left\{1 + \frac{b}{3}(\cos\alpha - 1) - \sqrt{-1}\ \theta_1 p\bar{A}\sin\alpha\right\}}. \tag{2.14}$$

$\bar{A}$ is equivalent to the locally constant value of $A(u) = \partial f/\partial u$ in the system

$$\frac{\partial u}{\partial t} + \bar{A}\frac{\partial u}{\partial x} = 0. \tag{2.15}$$

$\alpha = \beta h$, β is the variable in the Fourier space. Let $g(\alpha)$ denote the eigenvalue of $G(\alpha)$ and let the real number λ be an eigenvalue of $\bar{A}$. After some simplification,

$$|g(\alpha)|^2 = 1 - \frac{2acp^2\lambda^2\left[\frac{2b}{3} - 1 - 2acp^2\lambda^2\right]\left[1 - \cos\alpha\right]^2}{\left[1 + \frac{b}{3}(\cos\alpha - 1)\right]^2 + \theta_1^2 p^2\lambda^2\sin^2\alpha}. \tag{2.16}$$

When $b = 0$, $c = -d$ and $\theta_1 = -2b$, Eq. (2.16) gives the relation obtained by McGuire and Morris [9] for their general scheme. From (2.14), the matrix $G(\alpha)$ can be diagonalized since $\bar{A}$ has a complete set of linearly independent eigenvectors. Thus, the Von Neuman condition is sufficient as well as necessary for the stability of the scheme [13]. The stability, in the linearized sense, is assured provided

$$0 \leqslant 2\,acp^2\lambda^2, \qquad \frac{2b}{3} - 1 - 2acp^2\lambda^2 \leqslant 1 \tag{2.17}$$

for a, $c > 0$ and for all the eigenvalues λ of $\bar{A}$. The corresponding condition for the stability, when $a > 0$ and $c < 0$ is given by

$$-1 \leqslant 2acp^2\lambda^2, \qquad \frac{2b}{3} - 1 - 2acp^2\lambda^2 \leqslant 0. \tag{2.18}$$

In order to obtain the dissipative schemes, we neglect the equality sign in (2.17) and (2.18). Then there exists a constant $\delta_1 > 0$ such that

$$|g(\alpha)| \leqslant 1 - \delta_1|\alpha|^4 \tag{2.19}$$

for all eigenvalues g of G and for all $|\alpha| \leqslant \pi$. Inequality (2.19) shows that the scheme (2.17) is dissipative and of order four in the linearized sense. Inequalities (2.17) and (2.18) are the conditions for the choice of the mesh ratio p and parameter b. In the case of a dissipative scheme, these conditions are given by

$$p\,|\lambda| < 1/(2ac)^{1/2}, \tag{2.20}$$

$$3(1+2acp^2\,|\lambda|^2)/2 < b < 3(1+acp^2\,|\lambda|^2), \tag{2.21}$$

provided $c > 0$, $a > 0$ and $\lambda \neq 0$ and

$$-1 < 2acp^2\,|\lambda|^2 < 0, \tag{2.22}$$

$$3acp^2\,|\lambda|^2 < b < 3(1+2acp^2\,|\lambda|^2)/2, \tag{2.23}$$

when $a > 0$ and $c < 0$.

Scheme (2.7) yields a nonlinear system of difference equations. Instead of using iterative methods which are time-consuming, we have used the technique followed by Gourlay and Morris [5] for solving the implicit nonlinear equations; this technique gives rise to a block tridiagonal system at each time level. Let the matrix $\widetilde{A}$ be defined by

$$f(u) = \widetilde{A}(u)\cdot u\,. \tag{2.24}$$

The choice of $\widetilde{A}$ will depend on the particular problem to be solved. Using (2.24) and (2.7), one gets

$$\left\{1+\frac{b}{6}\delta_x^2-\frac{p}{2}\theta_1\mu\delta\widetilde{A}(W_i^{n+1})\right\}W_i^{n+1}$$
$$=\left\{(1+\frac{b}{6}\delta_x^2)W_i^n+\frac{b}{2}\theta_2\mu\delta f_i^n+pc(\overset{*}{f}{}_{i+\frac{1}{2}}^{n+a}-\overset{*}{f}{}_{i-\frac{1}{2}}^{n+a})\right\}. \tag{2.25}$$

Let W_i^{**n+1} denote an approximation for $u\,(ih,(n+1)k)$ which is at least of first-order accuracy and is smooth through the second-order terms. McGuire and Morris [9] have shown that the replacement of $\widetilde{A}\,(W_i^{n+1})$ by $\widetilde{A}\,(W_i^{**n+1})$ does not alter the second-order accuracy of the method. We have used Eq. (2.7) with $\theta_1 = 0$ and $b = 0$ to determine W_i^{**n+1} with the proper choice of the parameters θ_2, a, c from Eqs. (2.10) and (2.11) to get the second-order accuracy of W_i^{n+1}. Thus Eq. (2.25) yields a three-block recurrence relation at each time level. We require W_o^{n+1} and W_N^{n+1} at the boundaries for solving it. At the lower boundary, we can take $W_o^n = u_1(nk)$, $n = 1,2,\ldots$. There are two methods for calculating W_N^{n+1}. First, we can calculate W_N^{n+1} by one of the many available explicit techniques. This approach gives a block tridiagonal system to be solved at each time level for $\{W_i^n\}_i^{N-1}$. The second approach is to replace the operator δ_x^2 and $\mu\delta$ in Eqs. (2.7) to (2.9) by ∇_x^2 and $2\,\nabla_x+\nabla_x^2$; it gives a block tridiagonal system for $\{W_i^n\}_i^{N-1}$ at each time level [9]. We have used the second approach for our computational work.

3. Test examples

EXAMPLE 1:

Consider the scalar equation

$$\frac{\partial u}{\partial t} + \frac{\partial}{\partial x}(u^2/2) = 0 \tag{3.1}$$

over the region R for the initial and boundary conditions

$$u_0(x) = x^2, \qquad u_1(t) = 0. \tag{3.2}$$

Its exact solution is given by

$$u(x, t) = [1 + 2xt - (1 + 4xt)^{1/2}]/2t^2. \tag{3.3}$$

Using inequalities (2.21) and (2.23),

$$b \in [1.5, 4.5], \quad \text{if } a > 0, \quad c > 0, \tag{3.4}$$

and

$$b \in [-1.5, 1.5], \quad \text{if } a > 0, \quad c < 0. \tag{3.5}$$

For $b \in [1.5, 4.5]$, the elements along the principal diagonal of the matrix take very small values and for $b = 3$ they are all zero. This gives rise to difficulties in the solution of the matrix equation. We have considered the case when $b \in [-1.5, 1.5]$. Table I provides a summary of the errors for this problem at the 300th time step. The stability condition is $ac \in [-0.5, 0]$ when $p = 1$. By examining the numerical results, one finds that the schemes are stable for $ac \in [-d, 0]$, where the value of d is larger than predicted by the linearized theory. The same remark holds good when $p = 2.0$, but the instability occurs for smaller values of $|ac|$ compared with the corresponding value when $p = 1.0$. The errors are found to be smaller for the case when the parameters satisfy the relations (2.10) to (2.13). To be specific, the errors are small for $b = 0.5$, $a = 0.90825$, $c = -2.0$ and $b = 0.5$, $a = 0.5$, $c = 0.6667$.

EXAMPLE 2:

Consider Eq. (3.1) with the discontinuous initial data

$$u_0(x) = \begin{cases} 1, & 0 \leqslant x < 0.1 \\ 0, & x \geqslant 0.1 \end{cases}$$

and the boundary data

$$u_1(t) = 1, \quad t > 0.$$

TABLE I

Error $E \cdot 10^6$ at the 300th time step at the central grid point for Example 1

	a \ c	−0.125	−0.25	−0.5	−1.0	−2.0	−4.0
	0.125	−993	−896	−726	−492	−133	486
	0.25	−782	−739	−648	−471	−138	480
$p = 1.0$	0.50	−636	−655	−618	−476	−150	462
$b = -0.5$	1.00	−612	−659	−629	−483	−179	417
	2.00	−681	−626	−647	−515	−244	300
	4.00	−715	−703	−683	−586	−359	*
		$a = 0.90825$,		$c = -2.0$,		$E \cdot 10^6 = -173$	
	0.125	−138	−199	−270	−273	−75	329
	0.25	−1215	−839	−480	−309	−81	325
$p = 2.0$	0.50	−1513	−869	−448	−322	−95	311
$b = -0.5$	1.00	−981	−547	−438	−340	−124	289
	2.00	−506	−493	−457	−375	−212	144
	4.00	−592	−505	−439	*	*	*
		$a = 0.92825$,		$c = -2.0$,		$E \cdot 10^6 = -118$	
	0.125	132	34	−16	79	395	972
	0.25	−106	−106	−71	66	391	961
$p = 1.0$	0.50	−265	−187	−101	55	380	958
$b = 0.5$	1.00	−295	−201	−113	40	357	930
	2.00	−255	−200	−130	11	303	852
	4.00	−252	−218	−161	−52	194	*
		$a = 0.5$,		$c = -0.6667$,		$E \cdot 10^6 = -50$	

* Instability

TABLE II

Values of the parameters for the scheme (2.7) to be stable for Example 2

($b = -0.5, 0.5$)

	$b = -0.5$		$b = 0.5$	
p	c	Maximum value of $a > 0$ for stability	c	Maximum value of $a > 0$ for stability
1.0	−0.125	4.0	−0.125	2.0
	−0.25	2.0	−0.25	1.0
	−0.50	1.0	−0.50	0.5
	−1.0	0.5	−1.0	0.25
	−2.0	0.25		
2.0	−0.125	1.0	$c = -0.6667$	$a = 0.5$
	−0.25	0.5		
	−0.50	0.25		

The solution of this problem has a discontinuity travelling into the field of solution along the line $x = 0.1 + t/2$ with velocity $\partial x/\partial t = 0.5$. In Fig. 1, we have drawn curves for the solution given by the difference scheme (2.7) after the 50th time step for the grid points between $x = 25\,ph$ and $x = 25\,ph + 15\,h$. The theoretical shock occurs at the grid point $x = 25\,ph + 10\,h$. In all cases, we have chosen $h = 0.01$. Table II gives the values of the parameters for the region of stability when $b = -0.5$, 0.5 and $p = 1.0$, 2.0. On examining Fig. 1 and the computed results, one finds that the 'best' shock profiles are obtained for parameter values close to the maximum values predicted by the stability conditions. For $p = 1.0$ and $b = 0.5$, the 'best' profiles are derived for the values $|ac| \cong 0.5$ and for the parameters satisfying the relations (2.10) to (2.13).

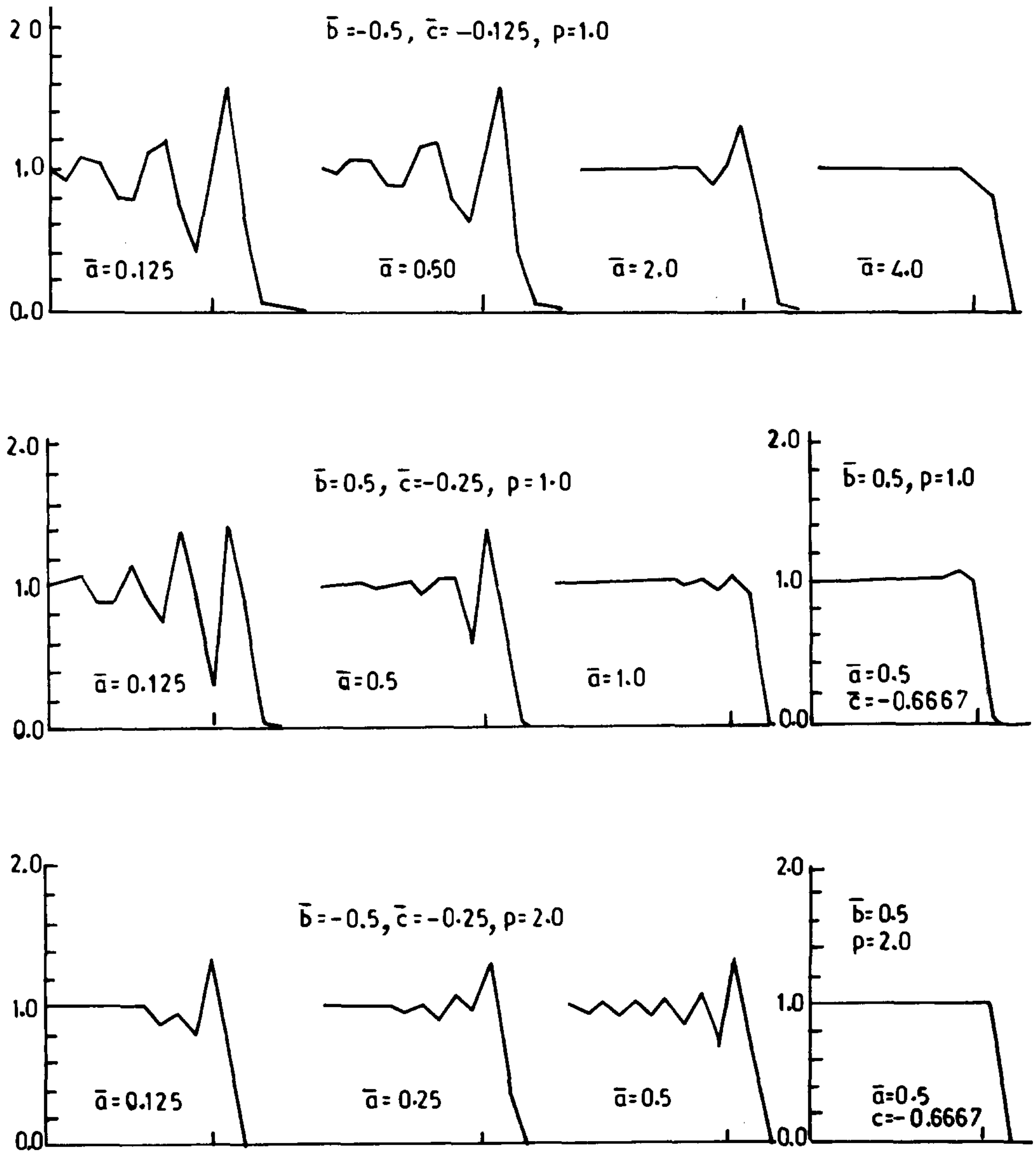

Figure 1. Solution of Example 1 at 50 Δt by scheme (2.7)

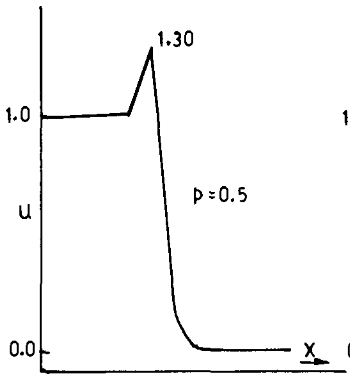

Figure. 2. Solution of Example 2 by the Lax-Wendroff scheme

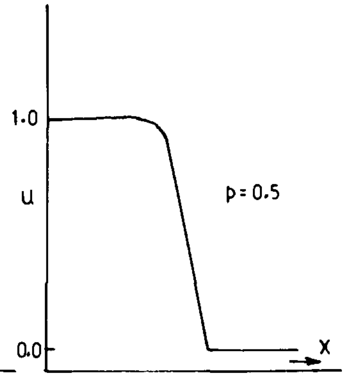

Figure 3. Solution of Example 2 by the MacCormack method

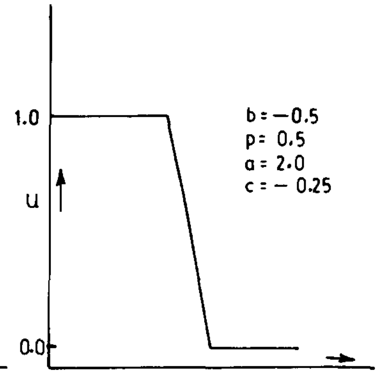

Figure 4. Solution of Example 2 by scheme (2.7)

Figs. 2, 3 and 4 show shock profiles as obtained by using the Lax-Wendroff method, the MacCormack method and our method respectively. The comparison of these figures shows that the proposed technique gives better shock profiles for certain values of the parameters.

4. The filter technique

By numerical experiments, we get shock profiles with oscillations when the parameters are such that they satisfy inequality (2.17) close to the lower bound. To minimise these undesirable oscillations for the chosen values of the parameters, we use the automatic switched Shuman-filter technique [16]. From Eq. (2.16), it is observed that the scheme does not have dissipation for the following cases:

$$acp^2\lambda^2 = 0, \tag{4.1}$$

$$\frac{2b}{3} - 1 - 2acp^2\lambda^2 = 0, \tag{4.2}$$

$$\cos\alpha - 1 = 0. \tag{4.3}$$

It may be remarked that conditions (4.1) and (4.2) cannot be considered when the parameters satisfying these conditions violate the condition of dissipation. For the wave length $L = \Delta x$ and using the relation $L/\Delta x = 2\,\pi/\alpha$, it is found that no damping occurs in this case. To avoid this type of situation, we use the relation

$$\tilde{W}_i^{n+1} = W_i^n + \frac{1}{4}\left[\tilde{\theta}^{n+1}_{i+\frac{1}{2}}\,(W^{n+1}_{i+1} - W^{n+1}_i) - \tilde{\theta}^{n+1}_{i-\frac{1}{2}}\,(W^{n+1}_i - W^{n+1}_{i-1})\right], \tag{4.4}$$

where $\tilde{\theta}$ is the automatic switch to be defined later. Using Taylor series expansion, the right-hand side of Eq. (4.4) approximates $\left[W + \frac{1}{4}h(\tilde{\theta}W_x)_x\right]_i^{n+1}$ which is in conservation form.

We treat $\widetilde{\theta}$ as a local constant and use the Fourier transform method on Eq. (4.4) to get

$$S = \left(1 - \widetilde{\theta} \sin^2 \frac{\xi}{2}\right) I,$$

where S is the amplification matrix corresponding to the filtering step (4.4). Vliegenthart [15] and Harten and Zwas [14] have shown that S has a damping effect and the phases of the Fourier components are unaffected as S is a real quantity. It can be shown that if $0 \leqslant \widetilde{\theta} \leqslant 2$, then for every ξ, $|\xi| \leqslant \pi$,

$$\left| 1 - \theta \sin^2 \frac{\xi}{2} \right| \leqslant 1.$$

Hence, the stability condition remains unaltered.

The automatic switch $\widetilde{\theta}$ in Eq. (4.4) is defined to satisfy the following properties:

(i) Representation in conservation form.
(ii) Preservation of the linear stability of the basic scheme.
(iii) Sensibility to shock-like discontinuities ($\widetilde{\theta} = O(1)$ at the shock).
(iv) Absence of effect on the accuracy in smooth regions ($\widetilde{\theta} = O(h^{r-1})$).

Conditions (i) and (ii) are already satisfied.

One can construct a function of the dependent variables which is a good sensor for shocks. We consider two such functions containing λ, the largest eigenvalue of $A = A(u)$,

$$\widetilde{\theta}_{i+\frac{1}{2}} = \chi \left(\frac{\lambda_{i+1} - \lambda_i}{\operatorname{Max}_l |\lambda_{l+1} - \lambda_l|} \right)^m, \tag{4.5}$$

$$\widetilde{\theta}_{i+\frac{1}{2}} = \chi \exp \left\{ 1 - \left(\frac{\operatorname{Max}_l |\lambda_{l+1} - \lambda_l|}{\lambda_{i+1} - \lambda_i} \right)^m \right\}, \tag{4.6}$$

where $m \geqslant r - 1$ (r is the order of accuracy of the scheme), $\chi = 2/D$, (D is the space dimension). Computationally, we have found that the best results are obtained for $1/2 \leqslant \chi \leqslant 1$. The function $\widetilde{\theta}$ in (4.5) is an adequate sensor for the shock region but can be dangerous for the following cases:

(1) The solution is to be continuous and the desired order of accuracy of the basic scheme is to be maintained everywhere.
(2) When the solution contains rarefaction in addition to shocks.

In these cases, it is better to use the second function $\widetilde{\theta}$ as given by (4.6).

We have solved two examples for testing the validity of the above-defined filter for handling the discontinuities.

EXAMPLE 3:

$$u_t + uu_x = 0$$

with the initial conditions

$$u_0(x) = \begin{cases} 2 & , x < 0.1 \\ 0 & , x \geqslant 0.1 \end{cases}$$

or

$$u_0(x) = \begin{cases} 1 & , x \leqslant 0 \\ 1 - x & , 0 \leqslant x \leqslant 1 \\ x - 1 & , 1 \leqslant x \leqslant 2 \\ 1 & , 2 \leqslant x \end{cases}$$

In the latter case, a shock will be formed at time $t = 1$, and there will be a rarefaction region with gradients decreasing with time t. In this case, the exact solution in the continuous region $(0 \leqslant t < 1)$ is

$$u(x, t) = \begin{cases} 1 & , x \leqslant t \\ \dfrac{1-x}{1-t}, & t \leqslant x \leqslant 1 \\ \dfrac{x-1}{t+1}, & 1 \leqslant x \leqslant 2 + t \\ 1 & , 2 + t \leqslant x \end{cases}$$

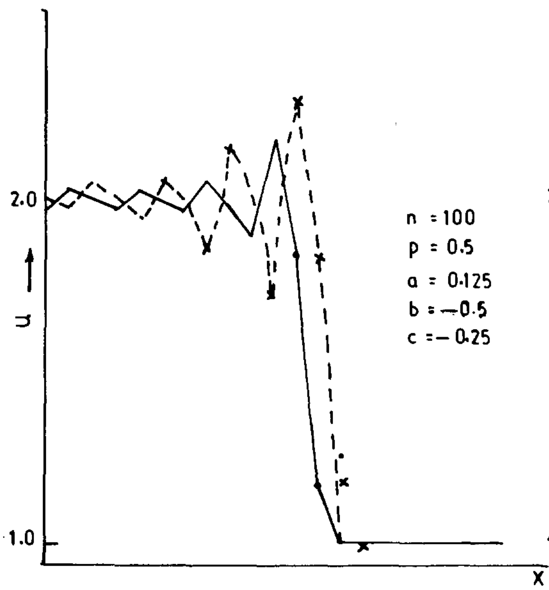

Figure 5a. Solution of Example 3 by scheme (2.7)
– – – – – without filter
———— with filter

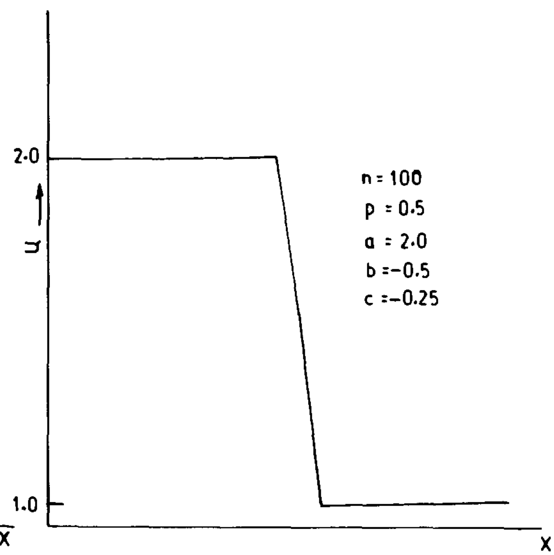

Figure 5b. Solution of Example 3 by the proposed scheme using filter

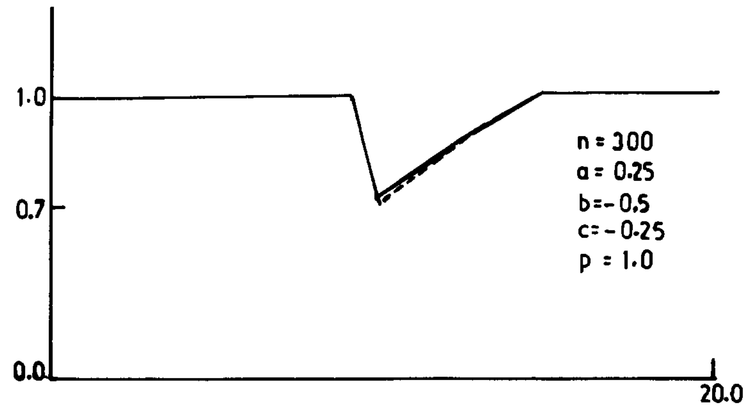

Figure 6. Comparison of solutions:
——— With filter
– – – – Exact solution

In the discontinuous region ($1 \leqslant t$), the solution is

$$u(x, t) = \begin{cases} 1 & , x < 2 + t - \tau \qquad \text{where } \tau = (2 + 2t)^{1/2} \\ \dfrac{x-1}{t+1} & , 2 + t - \tau \leqslant x \leqslant 2 + t \\ 1 & , 2 + t \leqslant x \end{cases}$$

From Fig. 5a, it is seen that the oscillations are reduced when we use the automatic Shuman filter in the computational scheme. We have drawn the graph for those parameters which give large oscillations compared to the other values of the parameters. It may be remarked that it is possible to obtain a solution with almost no oscillations and sharp profiles by using the switched filter as shown in Fig. 5b for certain values of the parameters. From Fig. 5b, it may be noted that the discontinuity is displaced to the right by two mesh points because of the dissipative character of the scheme.

Fig. 6 shows the superiority of the automatic-switch-filter technique for solving those problems whose solutions contain rarefaction in addition to shocks.

5. The two-dimensional case

We consider the system of conservation laws in two space dimensions

$$\frac{\partial u}{\partial t} + \frac{\partial f}{\partial x} + \frac{\partial f}{\partial y} = 0 \tag{5.1}$$

defined on the region D given by

$$D = [0, X] \times [0, Y] \times [t > 0]$$

with appropriate initial and boundary conditions. We have extended the method proposed in Section 2 for the one-dimensional case by making use of the Strang [16] formulation. We illustrate the method by an example.

EXAMPLE 4:
Consider the equation

$$\frac{\partial u}{\partial t} + \frac{\partial}{\partial x}(u^2/4) + \frac{\partial}{\partial y}(u^2/4) = 0 \tag{5.2}$$

with the initial and boundary conditions

$$u(x, y, 0) = (x+y)^2/4, \tag{5.3}$$

$$u(0, y, t) = \{[1-(1+yt)^{1/2}]/t\}^2, \tag{5.4}$$

$$u(x, 0, t) = \{[1-(1+xt)^{1/2}]/t\}^2. \tag{5.5}$$

The exact solution of the problem defined on the region

$$D = (0,1) \times (0,1) \times (t > 0)$$

is given by

$$u(x, y, t) = \{[1-(1+(x+y)\,t)^{1/2}]/t\}^2.$$

TABLE III

Error E . 10⁶ after 300 time steps at the central grid point for Example 4

	a \ c	−0.125	−0.25	−0.50	−1.0	−2.0	−4.0	−8.0
	0.125	−531	−505	−451	−343	−125	315	1194
	0.25	−538	−510	−454	−343	−120	324	1244
	0.50	−542	−513	−455	−342	−117	330	1237
$p = 1.0$	1.00	−543	−513	−454	−341	−121	325	1263
$b = -0.5$	2.00	−542	−513	−458	−355	−152	277	1127
	4.00	−546	−525	−496	−427	−292	−30	−466
	8.00	−575	−592	−636	−724	−974	−1815	−3485
	16.00	−715	−881	−1266	−1998	−3516	*	*
		$a = 0.90825$,		$c = -2.0$,		$E \,.\, 10^6 = -120$		
	0.125	−788	−717	−593	−397	−128	219	772
	0.25	−943	−834	−652	−391	−90	251	820
$p = 4.0$	0.50	−988	−829	−589	−300	−39	269	*
$b = -0.5$	1.00	−855	−662	−416	−199	−32	276	*
	2.00	−564	−420	−283	−198	−86	*	*
	4.00	−274	−306	−316	−310	−324	*	*

* Instability

In Table III, errors are given for the same values of the parameters as for the one-dimensional problem. On examining the computed results, one finds the behaviour of the solutions for the two-dimensional case to be similar to the one-dimensional case. For example, it is seen that the stability (at least for the 50th time step) holds over a larger range than given by the theoretical value for $p = 1.0$ and $p = 4.0$. The errors become smaller for the parameters satisfying the relations (2.10) to (2.13); for example, $b = -0.5$, $a = 0.90825$, $c = -2.0$ and $b = 0.5$, $a = 0.5$, $c = -0.6667$.

Hence, the cubic-spline-function technique can be used successfully for devising algorithms for the solutions of nonlinear system of conservation laws. This technique has also been used for the solution of nonlinear, coupled Burgers' equations at high Reynolds numbers [17].

Acknowledgement

The authors wish to express their gratitude to the Department of Atomic Energy, Government of India, for the financial support in the preparation of this paper. One of the authors (D.N.H.) is grateful to the Council of Scientific and Industrial Research for the award of Research Fellowship for undertaking this research work.

REFERENCES

[1] R. D. Richtmyer, A survey of difference methods for non-steady fluid dynamics, *N.C.A.R. Tech. Notes*, 63-2 (1962).
[2] A. R. Gourlay and J. Ll. Morris, Finite difference method for non-linear hyperbolic systems, *Math. Comp.* 22 (1968) 28-39.
[3] E. L. Rubin and S. Z. Burstein, Difference methods for the inviscid and viscous equations of a compressible gas, *J. Comp. Phys.* 2 (1967) 178-196.
[4] G. R. McGuire and J. Ll. Morris, A class of second-order accurate methods for the solution of systems of conservation laws, *J. Comp. Phys.* 11 (1973) 531-549.
[5] A. R. Gourlay and J. Ll. Morris, Finite difference methods for non-linear hyperbolic systems, *Math. Comp.* 22 (1968) 549-555.
[6] J. Gary, On certain finite difference schemes for hyperbolic systems, *Math. Comp.* 18 (1964) 1-18.
[7] S. Abarbanel and G. Zwas, An iterative finite difference method for nonlinear hyperbolic systems, *Math. Comp.* 23 (1969) 549-565.
[8] R. M. Beam and R. F. Warming, An implicit finite difference algorithm for hyperbolic systems in conservation law form, *J. Comp. Phys.* 22 (1976) 87-110.
[9] G. R. McGuire and J. Ll. Morris, A class of implicit, second-order accurate, dissipative schemes for solving systems of conservation laws, *J. Comp. Phys.* 14 (1974) 126-147.
[10] A. Jeffrey and T. Taniuti, *Nonlinear wave propagation*, Academic Press, New York (1964).
[11] I. J. Ahlberg, E. N. Nilson and J. L. Walsh, The theory of splines and their applications, *Academic Press*, New York (1967).
[12] A. Lerat and R. Peyret, *C.R. Acad. Sci. Paris* Ser. A-B 277 (1973) A363-A366.
[13] R. D. Richtmyer and K. W. Morton, *Difference methods for initial value problems*, Interscience, New York (1967).
[14] A. Harten and G. Zwas, Switched numerical Shuman filter for shock calculations, *J. Eng. Math.* 6 (1972) 207-216.
[15] A. C. Vliegenthart, The Shuman filtering operator and the numerical computation of shock waves, *J. Eng. Math.* 4 (1970) 341-348.
[16] W. G. Strang, On the construction and comparison of difference schemes, *SIAM J. Numer. Anal.* 5 (1968) 506-517.
[17] P. C. Jain and D. N. Holla, Numerical solution of coupled Burgers' equations (To appear in *International J. of Nonlinear Mechanics*).